Extremely Fast Tripping for an Arc-Flash Event: A Field Case Analysis

Manibhushan Prasad
Tata Power Delhi Distribution Limited

Mohanraj Perumalsamy, Shripad Kapse, Chethan Kumar Barikar,
Deepak Srivastava, and Ricardo Abboud
Schweitzer Engineering Laboratories, Inc.

Presented at the
46th Annual Western Protective Relay Conference
Spokane, Washington
October 22–24, 2019

Extremely Fast Tripping for an Arc-Flash Event: A Field Case Analysis

Manibhushan Prasad, *Tata Power Delhi Distribution Limited*
Mohanraj Perumalsamy, Shripad Kapse, Chethan Kumar Barikar, Deepak Srivastava, and Ricardo Abboud,
Schweitzer Engineering Laboratories, Inc.

***Abstract*—An arc-flash event is a dangerous release of energy caused by an electric arc. Across utilities and industries, the safety of personnel and equipment is of paramount importance. This safety is threatened by hazardous and potentially fatal arc-flash event effects, such as high levels of thermal and ultraviolet radiation, extreme blast pressure, deafening sound waves, and flying shrapnel. A fast fault-clearing time is crucial to minimizing arc-flash risks and damage, because the energy released during an arc flash is proportional to the event duration.**

In this paper, we describe an arc-flash event that occurred at the first 10 MW grid-tied energy storage plant in India, installed by Tata Power Delhi Distribution Limited (TPDDL) in New Delhi. The arc fault occurred during energization of the 415 V incomer breaker in a 66/11/0.415 kV distribution substation.

First, we explain arc-flash events and how to calculate associated incident energy. Next, we rank protection methods by how each reduces tripping times and incident energy. We discuss an arc-flash protection application that uses light sensors in conjunction with ultra-high-speed overcurrent elements, and we describe the design and deployment of that application at the TPDDL energy storage facility.

Finally, we analyze the arc-flash event that occurred at the TPDDL facility. We discuss the peak current values, the fast tripping time (3.76 ms) for the arc-flash system, and how the incident energy might have been reduced further if the inter-tripping scheme was in service at the moment of the fault. Inter-tripping schemes mitigate damage to personnel and equipment by allowing high-speed tripping to reduce arc-flash event boundary limits even when an arc-flash event evolves to include the incomer circuit breaker input terminals.

I. Introduction

Arc-flash incident energy is directly proportional to the voltage, current, and duration of the event (V • I • t). Event duration, or the operation time of the protection scheme, is the only controllable factor. Reducing operation time also reduces the arc-flash incident energy.

Engineers can apply different protection schemes and arc-flash detection technologies to reduce operation times. As we show in a field case analysis, one such arc-flash detection system installation mitigated an arc-flash event that occurred during the energization of a 415 V switchboard at an energy storage facility installed by Tata Power Delhi Distribution Limited (TPDDL) in New Delhi, India.

II. What is an Arc-Flash Event?

An arc-flash event is characterized by the conduction of electric current at high speeds through a normally nonconductive material, such as air. Faults that cause these events are associated with short circuits. Most arc-flash events are initiated by single-phase-to-ground faults or phase-to-phase faults that rapidly evolve to three-phase faults.

Arc-flash behavior is considered chaotic, because it involves a rapid and irregular change in arc geometry due to the electromagnetic forces involved in the phenomenon. The chaotic behavior makes it very difficult for engineers to model an arc-flash event.

III. Arc-Flash Incident Energy and Risks to Workers

A growing awareness of work safety issues, as well as an increase in strict safety and health standards, has led to important and beneficial changes in the electric industry regarding the design and operation of electrical installations. In new installations, correctly measuring risks and providing solutions to mitigate them are now fundamental steps that help ensure facility integrity and worker safety.

Among the hazards posed by electricity, an arc-flash event can be one of the most harmful to operating personnel. The National Fire Protection Association (NFPA) defines an arc-flash hazard as "a source of possible injury or damage to health associated with the release of energy caused by an electric arc" [1]. Workers can suffer serious and potentially fatal burns due to the large amount of energy released and the extremely high temperatures generated by an arc-flash event. In addition to high temperature, arc-flash event hazards include the ejection of toxic metal vapors, high-speed flying shrapnel, intense light, and a pressure wave caused by the expansion of gases. These effects can also cause considerable damage to electrical installations, such as the destruction of electrical panels.

In 2013, the Industrial Safety and Hygiene News Magazine compiled arc-flash event information and resulting injuries in the United States and published a summary list [2]. The list includes the following per-year estimates:

- Arc-flash incidents—30,000.
- Burn injuries—7,000.
- Hospitalizations—2,000.
- Fatalities—400.
- Percentage of electrical worker fatalities caused by burns, not shock—80 percent.

Worker or operator tasks that involve a significant possibility of an arc-flash event occurring are presented in [1] along with estimates of the likelihood of occurrence for each task. Some of these tasks include: opening doors or covers to expose energized conductors and circuits; working on such energized systems (including voltage testing); and removing or installing circuit breakers and switches.

Instantaneous heat energy measured at a certain distance from an arc flash is called incident thermal energy or simply incident energy. Incident energy is expressed in calories per square centimeter (cal/cm^2)—or, the heat energy impressed on an area measuring one square centimeter.

The amount of incident energy released by an arc-flash event depends on the following factors:

- Available short circuit current.
- System voltage.
- Arc gap.
- Total time to clear the fault (the protective relay tripping time plus the circuit breaker opening time).

To reduce injury from incident energy released in arc-flash events, workers and operators should wear personal protective equipment (PPE). Table I, adapted from [1], lists arc-flash PPE categories. These categories, based on calculated incident energy at working distance from an arc flash, detail the PPE that workers should wear to limit potential incident energy damage to a second-degree burn. (Additional PPE may be required, so engineers should consult [1] for the complete list.)

TABLE I
ARC-FLASH PPE CATEGORIES

Category	Minimum Arc Rating (cal/cm^2)	Minimum PPE Requirement (arc-rated clothing)*
1	4	Long-sleeved shirt and pants (or coverall) Face shield (or arc-flash suit hood)
2	8	Long-sleeved shirt and pants (or coverall) Face shield (or arc-flash suit hood) and balaclava
3	25	Long-sleeved shirt and pants (or coverall) Arc-flash suit jacket and arc-flash suit pants to fit minimum arc rating Arc-flash suit hood Gloves
4	40	Long-sleeved shirt and pants (or) coverall Arc-flash suit jacket and arc-flash suit pants to fit minimum arc rating Arc-flash suit hood Gloves

* All categories also include jacket, parka, rainwear, or hard-hat liner as needed.

Working in panels with calculated incident energy higher than 40 cal/cm^2 is only allowed when the electrical installation is de-energized, because no PPE is capable of offering adequate protection for workers at that incident energy level.

Methods of estimating incident energy for specific conditions are presented in Annex D of [1]. The results can vary drastically depending on the specific system parameters. An arc-flash event can produce different incident energy levels depending on whether the arc is in open air or confined in a switchgear.

One widely used method is based on IEEE 1584, IEEE Guide for Performing Arc-Flash Hazard Calculations [3]. This guide provides models and an analytical process to calculate predicted incident energy and the arc-flash boundary, defined as the distance from a possible arc-flash source at which the incident energy is calculated to be 1.2 cal/cm^2 (the amount of energy that can impart a second-degree burn).

IV. PROTECTION SCHEMES AND INSTALLATIONS THAT MITIGATE ARC-FLASH HAZARDS

Using PPE to avoid arc-flash burns should not be considered the only arc-flash protection option. Electrical installation design must also incorporate protections that can reduce arc-flash hazards.

The amount of incident energy that a worker or operator can be exposed to during an arc-flash event is directly proportional to the voltage, current, and duration of the event (V • I • t). Higher current and longer exposure time produces greater incident energy [4]. One variable that can be positively and effectively controlled is the time it takes for the protection system to detect and clear the fault (total fault-clearing time) [5]. In order to reduce the exposure time of workers to the incident energy and, consequently, reduce the need for heavy and uncomfortable PPE, special protection schemes can be deployed.

Special protection schemes that can be used to reduce incident energy by reducing the total fault-clearing time include the following:

- Fast bus trip schemes.
- Bus differential protection schemes.
- Maintenance mode protection schemes.
- Arc-flash detection technology combined with high-speed overcurrent elements.

A. Fast Bus Trip Schemes

Fig. 1 shows a double-bus arrangement for medium- and low-voltage installations that includes a combination of overcurrent feeder (51F), coupler (51C), and main bus (51M) relays.

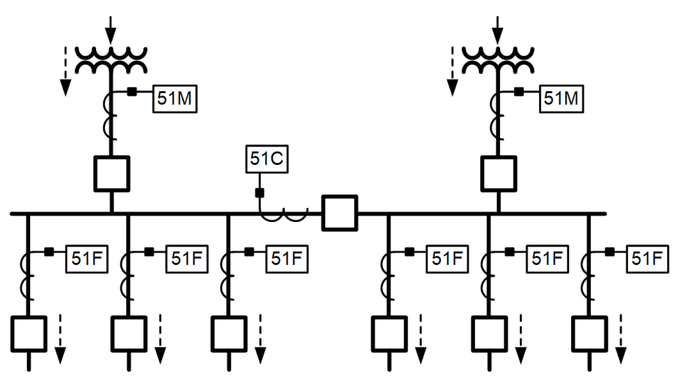

Fig. 1. Typical Double-Bus Configuration for Medium- and Low-Voltage Installations

A coordination interval between the tripping characteristics of series-overcurrent devices is mandatory to keep selectivity in a time-based coordination approach. This means that the 51C and 51M relays have a slow curve to coordinate with the slowest of the 51F relays. As shown in Fig. 2, this causes a long tripping time when there is a fault in the bus section. The goal of special protection schemes is to reduce the protection tripping time for a bus fault.

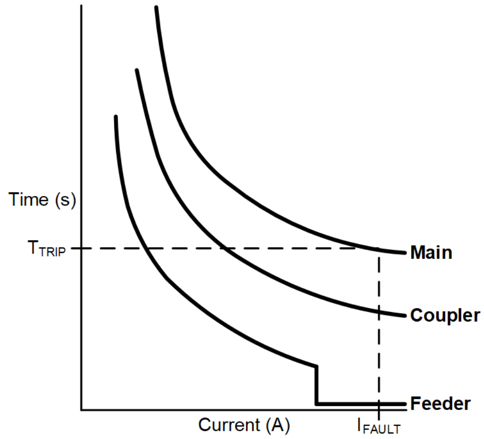

Fig. 2. Long Tripping Time for Bus Section Fault

The basic system model of a fast bus trip scheme, such as the one shown in Fig. 3, includes relays on the main and coupler breakers, 51M and 51C, that have a definite-time overcurrent element set with a time delay of about three cycles. When a fault occurs on a feeder, the 51F relay on that feeder detects the fault and sends a blocking signal to the 51C and 51M relays, preventing the operation of the fast definite-time overcurrent element.

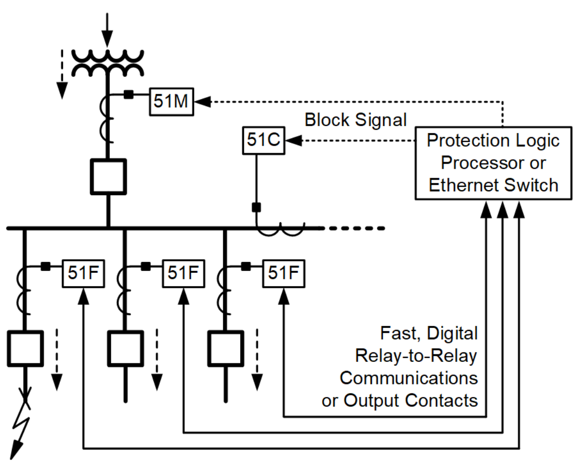

Fig. 3. Fast Bus Trip Scheme System Model With Fault on Feeder

For a fault on the bus, only the 51C and 51M relays detect the fault and a blocking signal is not received from any 51F feeder relay. As a result, the 51C and 51M relays clear the fault with the small (three-cycle) time delay. The traditional configuration with inverse-time overcurrent elements for the coordination of feeder faults is still in place, providing backup protection for feeder faults while still allowing for fast clearing times on bus faults.

The location of the feeder current transformers (CTs) is important for a fast bus trip scheme. A fast bus trip scheme covers internal breaker faults when the CTs are located on the load side of the breaker. This configuration differs from the systems shown in Fig. 1 and Fig. 3.

B. Bus Differential Protection Schemes

A low-impedance bus differential protection scheme operates based on the sum of the currents entering the bus, which is also called the differential current. The bus relay trips when it detects a differential current greater than a specified adaptive pickup [6].

Fig. 4 shows a typical connection setup for a system using a bus differential protection scheme. The cost to install a differential relay can be high, given the need for additional components including the relay, a panel or column, test switches, and cabling. However, the typical tripping time for a low-impedance differential protection scheme is only 1.25 cycles.

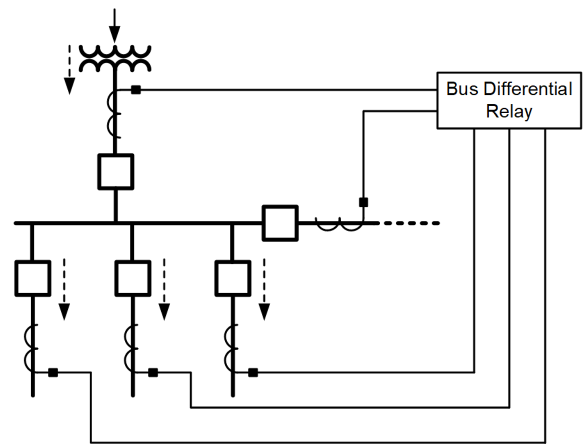

Fig. 4. Bus Differential Protection Scheme Connection Setup

C. Maintenance Mode Protection Schemes

To improve the safety of workers near energized equipment, some maintenance modes include an instantaneous overcurrent element for protection. The maintenance mode is manually enabled when personnel are within proximity of energized circuits (the hazard zone), and the mode can be enabled using a pushbutton on the relay, a separate switch, or a communication from a remote location.

While activated, the maintenance mode forces a change in protection scheme settings that disables the time coordination shown in Fig. 2 and allows the main breaker relay to trip without delay.

The main benefit of adding a maintenance mode protection scheme to a relay is faster tripping, which makes work conditions safer. An additional benefit is that such a scheme does not require much expense to implement for either old or new installations. At minimum, a switch and a small amount of wiring or logic is required.

However, there are also disadvantages to maintenance mode protection schemes. Coordination is lost, so the bus can be de-energized unnecessarily for a fault on the feeder. Human error is another concern: the switch for maintenance mode can be left on inadvertently, leaving workers vulnerable, or left off after maintenance is complete, rendering the whole protection system ineffective.

The typical tripping time for maintenance mode schemes is also about 1.25 cycles (the tripping time for the instantaneous overcurrent element).

D. Arc-Flash Detection Technology Combined With High-Speed Overcurrent Elements

A fault that includes an arc flash produces radiation that can be detected by a sensor. This allows engineers to implement arc-flash protection that operates based on the light emitted by the arc flash itself. Protective relays can incorporate arc-flash detection with inputs equipped for light sensors.

Combining light-based arc-flash detection with high-speed overcurrent elements allows for fast and secure tripping, because the two separate technologies detect faults independently, but detections from both are required for arc-flash protection tripping, as shown in Fig. 5.

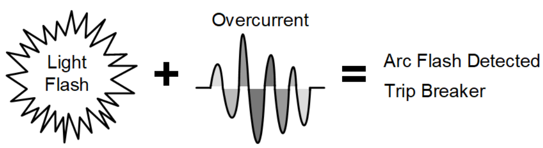

Fig. 5. Simple Combined Tripping Requirements in an Arc-Flash Protection Scheme

High-speed overcurrent protection elements prevent false, light-based trips, because the protection scheme also requires the elements to detect phase and neutral-ground overcurrent, so it does not trip a relay based on light detection alone.

A combined approach that uses a relay with arc-flash detection technology incorporated along with high-speed overcurrent elements is shown in Fig. 6.

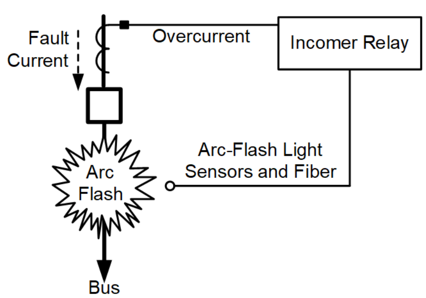

Fig. 6. Arc-Flash Detection Technology and Overcurrent Element Protection

Having arc-flash detection capabilities incorporated in the incomer relay confers several additional benefits, including the following:

- Fastest trip (2 ms) among all described methods.
- Maintained coordination between main (incomer) breaker and feeder for all operating conditions.
- Sensor health monitoring.
- Electrical isolation between light sensors and the relay location because of the fiber-optic cable connection.
- No need for additional copper wiring or CTs.

1) Using High-Speed Overcurrent Elements in Combined Approach

The overcurrent protection settings for relays in a distribution scheme are generally set with time coordination. This method allows enough time for the device closest to the fault to clear the fault before the next-closest device attempts to clear the fault. In this method, a time delay is added to each device to allow for time coordination. Typically these delays are around 0.3 seconds to provide a margin for the coordination. These delays are added to the trip times and can result in significant overall trip delay, raising the available incident energy in an arc-flash event.

a) Time Overcurrent Protection Example

To estimate the operate time for a relay with time overcurrent protection curves, this example applies a relay with a standard inverse curve setting and a time-multiplier setting (TMS) of 0.05. The relay operate time for a fault current that is ten times the set value in a 50 Hz system is 0.148 seconds. A sample circuit breaker operate time, based on typical data, is 0.06 seconds. The total time to clear the arc fault in this example is 0.148 seconds + 0.06 seconds = 0.208 seconds.

b) Instantaneous Overcurrent Protection Example

To estimate the operate time for a relay with instantaneous overcurrent protection, this example applies a relay with a standard operate time of 0.03 seconds in a 50 Hz system (it requires a sample from at least one complete cycle). The sample circuit breaker operate time of 0.06 seconds is used again. The total time to clear the arc fault is 0.03 seconds + 0.06 seconds = 0.09 seconds.

c) High-Speed Overcurrent Protection Example With Arc-Flash Detection System

This example assumes that the protective relay can differentiate an arc-flash fault within the switchgear from a fault outside the switchgear through the use of sensors. The sample circuit breaker operate time of 0.06 seconds is used. In the case of a detected arc fault, the relay operates in 5 ms or less. The total time to clear the arc fault in this example is 0.005 seconds + 0.06 seconds = 0.065 seconds.

2) Using Arc-Flash Detection Light Sensors in Combined Approach

Arc-flash detection technology uses two types of light sensors: point sensors, shown in Fig. 7a, and bare-fiber sensors, shown in Fig. 7b.

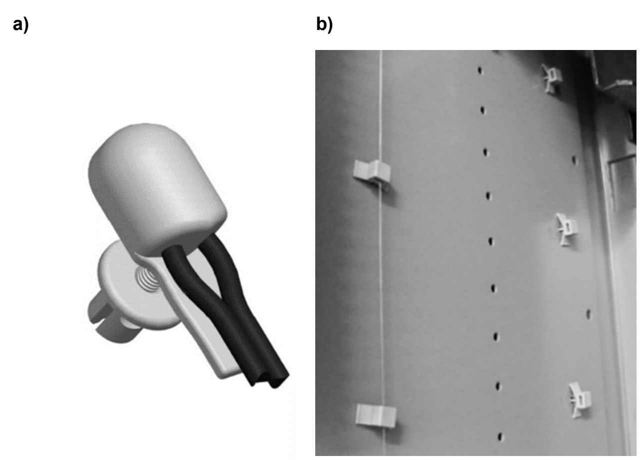

Fig. 7. Light Sensor Types Include a) Point Sensors and b) Bare-Fiber Sensors

Point sensors monitor confined spaces inside switchgears, where the distance between the sensors and any potential arc sources (energized parts) can be less than 2 meters. Typical application areas include compartments for breakers, outgoing and incoming cables, and potential transformers. Point sensors are flush-mounted on the switchgear cabinet wall using standard 1/4-inch holes, and then permanently fixed using mounting grommets or permanent cable ties.

Bare-fiber sensors monitor large, distributed resources, for example, switchgear system bus enclosures. Bare-fiber sensors are omnidirectional and can be mounted near switchgear enclosure walls. Bare-fiber sensors must be located within 2 meters of potential arc sources, with at least 0.5 meters of the fiber-optic cable exposed to the light from an arc flash.

The self-test function of any applied light sensors is important because of the critical nature of arc-flash protection. Protective relays should routinely test all connected light sensors. Reference [7] explains how to test light sensors in an arc-flash protection system.

3) *High-Speed Output Selection in Combined Approach*

To obtain faster arc-flash protection, engineers must select relay trip contacts with faster operating times. In some relays with arc-flash detection capabilities, designated outputs are available for high-speed processing (typically 1/16th of a cycle).

Fast hybrid outputs can also provide additional speed, and are rated for direct tripping of power circuit breakers. Typically, these high-speed, high-current-interrupting outputs can connect directly to circuit breaker trip circuits, operate in less than 50 µs, and have a breaking capacity of about 10 A (for an L/R of 20 ms or 40 ms). The dropout time for resistive load is 8 ms.

Engineers should implement high-speed, high-current-interrupting outputs as hybrid circuits. Each hybrid circuit consists of a parallel circuit of a high-current-rated solid-state switch and an electromechanical bypass relay. These hybrid output contacts can operate up to 8 ms faster than standard electromechanical outputs.

V. TPDDL Project Overview

TPDDL is a power distribution utility that operates in the north and northwest areas of Delhi, India. The utility covers a distribution area of 510 square kilometers, serving a population of 7 million and a customer base of 1.72 million, with a peak load of 2,063 MW. Additional operation figures include the following:

- Number of grid stations—80.
- Power transformer capacity—5,000 MW.
- Distribution transformer capacity—6,000 MW.
- Subtransmission network—150 circuits.

A. *TPDDL Objectives for the Energy Storage System*

As part of an initiative for new technology deployment, TPDDL proposed and implemented a 10 MW battery energy storage system in Sector 24, Rohini (Delhi), for a cost of about 7.5 million U.S. dollars. This particular substation was selected for the project because it feeds several hospitals and schools, which require an uninterrupted power supply.

In India, battery energy storage is in rising demand, given the maturity of the technology and the increasing energy usage throughout the country. The overall TPDDL objective for the battery energy storage project is to study the system network and analyze historical data, which will help the utility determine the potential energy storage capacity required to meet the peak load at that substation.

Subsequent objectives include: improving peak load management and frequency regulation; reducing penalties; deferring capital expenditure by avoiding network augmentation or addition of power-transforming equipment; accommodating and managing electric vehicle infrastructure growth; improving contingency services; and initiating the rollout of a “smart city” plan. For all of these goals, it is important for the utility to understand how to integrate energy storage into the whole configuration of the power system.

B. *Energy Storage System Overview*

Fig. 8 shows a one-line diagram of the system configuration.

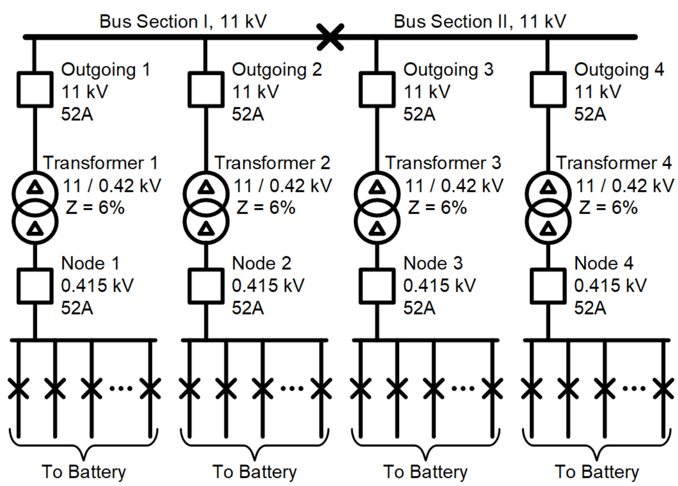

Fig. 8. One-Line Diagram of the 11/0.420 kV Switchboard

The substation has two 11 kV bus sections. Each bus section has two outgoing feeders, which are connected to isolation transformer feeders of 11/0.420 kV. The low-voltage side of each transformer is connected to the incomers of a battery node located inside the storage plant. Each node is used for charging and discharging a 2.5 MW battery section. There are a total of four battery nodes, resulting in a 10 MW total system capacity.

During off-peak times, the battery nodes use the grid power supply to charge the batteries. During peak load conditions, the energy stored in the batteries is used by the system to feed power back to the grid.

VI. Arc-Flash Hazard Calculations for the TPDDL Energy Storage System

The arc-flash incident energy and the arc-flash boundary are calculated using [3]. Analysis of the arc-flash intensity and arc-flash boundary in this section covers the 415 V bus side of Transformer 4 (see Fig. 8).

A. Bolted Fault Current

The first step in the arc-flash hazard calculations is to calculate the maximum available three-phase bolted fault current on the 415 V bus. The three-phase short-circuit current for the 11 kV bus (provided by TPDDL) is 10,747 A. Because both the X/R ratio for the source and the fault MVA are unknown, the source impedance in percent, $\%Z_{SOURCE}$, is calculated with (1) and the infinite-bus short-circuit calculation method is used to determine the maximum fault current on the secondary side of Transformer 4.

$$\begin{aligned}
\%Z_{SOURCE} &= \left(\frac{kVA_{TRANSFORMER}}{kVA_{SHORT_CIRCUIT}}\right) \bullet 100 \\
kVA_{SHORT_CIRCUIT} &= 10{,}747\ A \bullet 11\ kV \bullet \sqrt{3} \\
kVA_{SHORT_CIRCUIT} &= 204{,}757.9\ kVA \approx 204.76\ MVA \\
\%Z_{SOURCE} &= \left(\frac{2{,}500\ kVA}{204{,}757\ kVA}\right) \bullet 100 \\
\%Z_{SOURCE} &= 1.22
\end{aligned} \tag{1}$$

The maximum short-circuit current on the transformer 415 V bus (secondary), I_{BF}, is then calculated using (2), where $FLA_{SECONDARY}$ is the rated current for the secondary winding.

$$\begin{aligned}
I_{BF} &= \frac{FLA_{SECONDARY} \bullet 100}{\%Z_{TRANSFORMER} + \%Z_{SOURCE}} \\
I_{BF} &= \frac{3{,}436.61\ A \bullet 100}{6 + 1.22} \\
I_{BF} &= 47.598\ kA
\end{aligned} \tag{2}$$

B. Arcing Current

The arcing current, I_A, is also calculated at the 415 V bus using [3], as shown in (3).

$$\begin{aligned}
\log(I_A) = {} & K + 0.662 \bullet \log(I_{BF}) + 0.0966(V_{SYSTEM}) + \\
& 0.000526(G) + 0.5588\ V \bullet \log(I_{BF}) - \\
& 0.00304(G) \bullet \log(I_{BF}) \\
\log(I_A) = {} & -0.097 + 0.662 \bullet \log(47.598) + 0.0966(0.42) + \\
& 0.000526(32) + 0.5588\ V \bullet \log(47.598) - \\
& 0.00304(32) \bullet \log(47.598) \\
I_A = {} & 20.02\ kA
\end{aligned} \tag{3}$$

where:

I_A is the arcing current in kA.

I_{BF} is the low-voltage bus maximum fault current in kA.

K is resistance (–0.153 for open configuration, –0.097 for box configuration).

V_{SYSTEM} is the system voltage in kV.

G is the gap between conductors in mm.

C. Relay Operating Time

The operating time of the 415 V incomer relay for the arcing current is calculated as shown in (4). The calculation is based on the adaptive time overcurrent setting with inverse definite minimum time (IDMT) adopted in the applied relay, with an overcurrent pickup value (I_{PICKUP}) of 4,800 A primary and a TMS of 0.05, the setting for a standard inverse curve (C1).

$$\begin{aligned}
\text{Operating time} &= TMS \bullet \left(\frac{0.14}{\left[\frac{I_A}{I_{PICKUP}}\right]^{0.02} - 1}\right) \\
\text{Operating time} &= 0.05 \bullet \left(\frac{0.14}{\left[\frac{20.02\ kA}{4.8\ kA}\right]^{0.02} - 1}\right) \\
\text{Operating time} &= 0.242\ s
\end{aligned} \tag{4}$$

D. Comparison of Relay Operating and Fault-Clearing Times for Different Protection Schemes

Table II shows a comparison of three different protection schemes applied to the same 415 V incomer at Node 4 with an arcing current of 20.02 kA.

TABLE II
SETTINGS, RELAY OPERATING TIMES, AND FAULT-CLEARING TIMES AT 415 V INCOMER

Characteristic	Time Overcurrent Protection	Definite-Time Protection	Arc-Flash Detection System
Pickup value in primary amperes	4,800	5,600	5,600
Selected curve type	C1	NA	NA
Set delay or TMS	0.05	0.01	0.0
Operating time of relay in seconds	0.242	0.024	0.00376
Breaker opening time in seconds	0.06	0.06	0.06
Fault-clearing time in seconds	0.302	0.084	0.06376

E. Incident Energy

For buses in the range of 0.208 kV to 15.0 kV, the empirically derived method in [3] is used to calculate the arc-flash incident energy. The first step is to determine incident energy normalized for time and distance, and the second is to determine incident energy with specific parameters.

1) Normalized Incident Energy

The equation for normalized incident energy, (5), assumes a working distance of 610 mm and an arc duration of 0.2 s.

$$\begin{aligned}
\log(E_N) &= K_1 + K_2 + 1.081 \bullet \log(I_A) + 0.0011(G) \\
\log(E_N) &= -0.555 + 0 + 1.081 \bullet \log(20.02) + 0.0011(32) \\
E_N &= 7.71\ J/cm^2 \\
E_N &= 1.84\ cal/cm^2
\end{aligned} \tag{5}$$

where:

E_N is the incident energy normalized for time and distance in cal/cm^2 (converted from J/cm^2).

K_1 is resistance (–0.792 for open configuration, –0.555 for box configuration).

K_2 is resistance (0 for ungrounded and high-resistance grounded systems, –0.113 for grounded systems).

G is the gap between conductors in mm.

2) *Calculated Incident Energy With Parameters*

The normalized incident energy is then used to estimate the incident energy at a normal surface at a given distance and arcing time. The calculation in (6) is used for an arc-flash event at the 415 V breaker operating on standard inverse IDMT protection. This calculation can be applied to other system configurations as well.

$$\begin{aligned} E &= 4.184 \bullet C_F \bullet E_N \bullet \left(\frac{t}{0.2}\right) \bullet \left(\frac{610}{D}\right)^x \\ E &= 4.184 \bullet 1.5 \bullet 7.71 \bullet \left(\frac{0.302}{0.2}\right) \bullet \left(\frac{610}{610}\right)^{1.473} \\ E &= 73.068 \text{ J/cm}^2 \\ E &= 17.46 \text{ cal/cm}^2 \end{aligned} \tag{6}$$

where:

E is the incident energy in cal/cm^2 (converted from J/cm^2).

C_F is the calculation factor (1 for voltage greater than 1 kV, 1.5 for voltage of 1 kV or less).

t is the arcing time in seconds.

D is the working distance from the arc (the distance between the arc-flash point and the worker's face and torso) in mm.

x is the distance exponent.

Table III, adapted from [3], shows the distance exponent for several different configurations.

TABLE III
DISTANCE EXPONENT FOR VARIOUS VOLTAGES AND ENCLOSURE TYPES

Enclosure Type	0.208 to 1 kV	>1 to 15 kV
Open air	2	2
Switchgear or panel	1.473	0.973
Motor control center or power motor control center	1.641	NA
Cable	2	2

Table IV compares the incident energy for a definite-time protection scheme and an arc-flash detection system, calculated using (6) and the fault-clearing times from Table II.

TABLE IV
INCIDENT ENERGY FOR DIFFERENT PROTECTION SCHEMES

Protection Scheme	Fault-Clearing Time (s)	Incident Energy (cal/cm^2)
Definite-time protection at 415 V incomer	0.084	4.85
Arc-flash detection system at 415 V incomer	0.06376	3.68

F. *Arc-Flash Boundary*

The arc-flash boundary is the distance from an arc-flash source at which the incident energy is calculated to be 1.2 cal/cm^2 (the amount of energy that can impart a second-degree burn), and is calculated for a standard inverse IDMT operation of a 415 V breaker as shown in (7).

$$\begin{aligned} D_B &= 610 \bullet \left[4.184 \bullet C_F \bullet E_N \bullet \left(\frac{t}{0.2}\right) \bullet \left(\frac{1}{E_B}\right)\right]^{\frac{1}{x}} \\ D_B &= 610 \bullet \left[4.184 \bullet 1.5 \bullet 7.71 \bullet \left(\frac{0.302}{0.2}\right) \bullet \left(\frac{1}{5}\right)\right]^{\frac{1}{1.473}} \\ D_B &= 3{,}767.645 \text{ mm} \\ D_B &\approx 3.76 \text{ m} \end{aligned} \tag{7}$$

where:

D_B is the distance between the boundary and the arcing point in mm.

C_F is the calculation factor (1.5 for voltage of 1 kV or less).

E_N is the normalized incident energy in J/cm^2.

E_B is the incident energy at D_B in J/cm^2.

t is the arcing time in seconds.

x is the distance exponent (1.473 for switchgear or panel at a voltage of 1 kV or less).

Table V compares the arc-flash boundaries for a definite-time protection scheme and an arc-flash detection system, calculated using (7) and the fault-clearing times from Table II.

TABLE V
ARC-FLASH BOUNDARIES FOR DIFFERENT PROTECTION SCHEMES

Protection Scheme	Fault-Clearing Time (s)	Arc-Flash Boundary (m)
Definite-time protection at 415 V incomer	0.084	1.58
Arc-flash detection system at 415 V incomer	0.06376	1.31

G. *Incident Energy and Arc-Flash Boundary for the TPDDL System Arc-Flash Event*

To calculate the incident energy and the arc-flash boundary, the arc current value I_A is replaced by the recorded fault current from the field event, I_F, which is 39.88 kA.

The total fault-clearing time from the event is also used, which is calculated by adding the recorded relay operating time, 0.15306 s, to the recorded breaker operating time, 0.038 s, resulting in a total time of 0.19106 s (approximately 0.191 s for the purpose of the calculation).

Using the equation from (5), the normalized incident energy is calculated as shown in (8).

$$\begin{aligned} \log(E_N) &= K_1 + K_2 + 1.081 \bullet \log(I_A) + 0.0011(G) \\ \log(E_N) &= -0.555 + 0 + 1.081 \bullet \log(39.88) + 0.0011(32) \\ E_N &= 16.205 \text{ J/cm}^2 \end{aligned} \tag{8}$$

Then, using the equation from (6), the field event incident energy is calculated as shown in (9).

$$E = 4.184 \cdot C_F \cdot E_N \cdot \left(\frac{t}{0.2}\right) \cdot \left(\frac{610}{D}\right)^x$$

$$E = 4.184 \cdot 1.5 \cdot 16.205 \cdot \left(\frac{0.191}{0.2}\right) \cdot \left(\frac{610}{610}\right)^{1.473} \quad (9)$$

$$E = 97.16 \text{ J/cm}^2$$

$$E = 23.22 \text{ cal/cm}^2$$

Finally, using the equation from (7), the field event arc-flash boundary is calculated as shown in (10).

$$D_B = 610 \cdot \left[4.184 \cdot C_F \cdot E_N \cdot \left(\frac{t}{0.2}\right) \cdot \left(\frac{1}{E_B}\right)\right]^{\frac{1}{x}}$$

$$D_B = 610 \cdot \left[4.184 \cdot 1.5 \cdot 16.205 \cdot \left(\frac{0.191}{0.2}\right) \cdot \left(\frac{1}{5}\right)\right]^{\frac{1}{1.473}} \quad (10)$$

$$D_B = 4{,}571.862 \text{ mm}$$

$$D_B \approx 4.57 \text{ m}$$

The same process can calculate the incident energy and arc-flash boundary for the field event if an inter-tripping scheme had been active at the time. With a fault-clearing time of 0.0417 s and the recorded fault current of 39.88 kA, the incident energy E is 5.07 cal/cm^2 (converted from 21.22 J/cm^2) and the arc-flash boundary D_B is 1.62 m.

VII. Arc-Flash Detection System Design at the TPDDL Facility

Four outgoing switchgear panels are located in the 11 kV portion of the TPDDL facility. Each outgoing switchgear panel includes six point sensors installed for arc-flash detection in different compartments as follows:

- Two point sensors are located in the breaker compartment.
- Two point sensors are located in the busbar section inside the bus compartment.
- Two point sensors are located in the outgoing cable section in the cable compartment.

The sensor arrangement for an 11 kV outgoing switchgear panel is shown in Fig. 9.

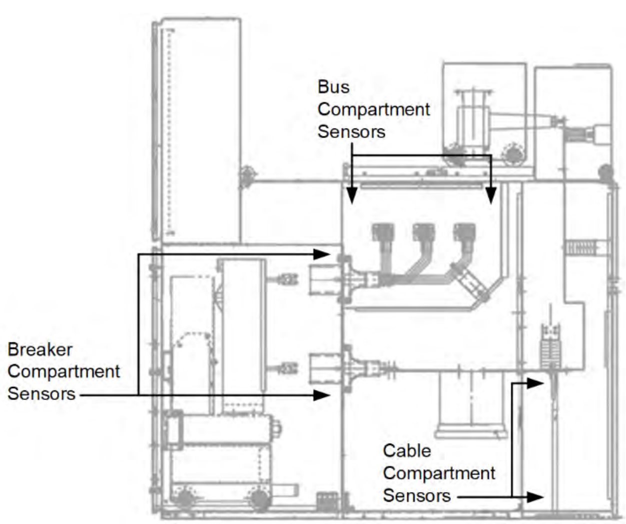

Fig. 9. Arc-Flash Detection Sensor Arrangement in Switchgear Panel

In the 415 V incomer switchgear, two point sensors and one bare-fiber sensor are installed for detecting the light from an arc-flash event.

In the same arc-flash detection system, a fast overcurrent detection element and a time-overlight (TOL) element are assigned to a fast, high-current-interrupting output contact in order to trip the circuit breaker directly, as shown in Fig. 10. This helps minimize fault-clearing time by eliminating the additional time associated with a lockout relay operation.

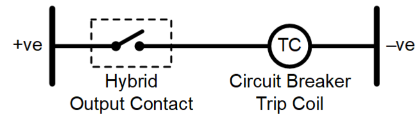

Fig. 10. Trip Circuit Configuration for Arc-Flash Detection Relay

A. 11 kV Switchgear Light Sensor Installation

Each 11 kV outgoing switchgear panel is connected to two relays that have arc-flash detection capabilities. Each compartment in the switchgear therefore includes two point sensors, with one point sensor connected to the first arc-flash detection relay and the other point sensor connected to the second arc-flash detection relay. This cross-connection configuration is designed to ensure reliable system operation. A total of 24 point sensors are installed in the four 11 kV outgoing switchgear panels.

Fig. 11 shows the locations where point sensors are installed in the breaker compartment of an 11 kV outgoing switchgear panel.

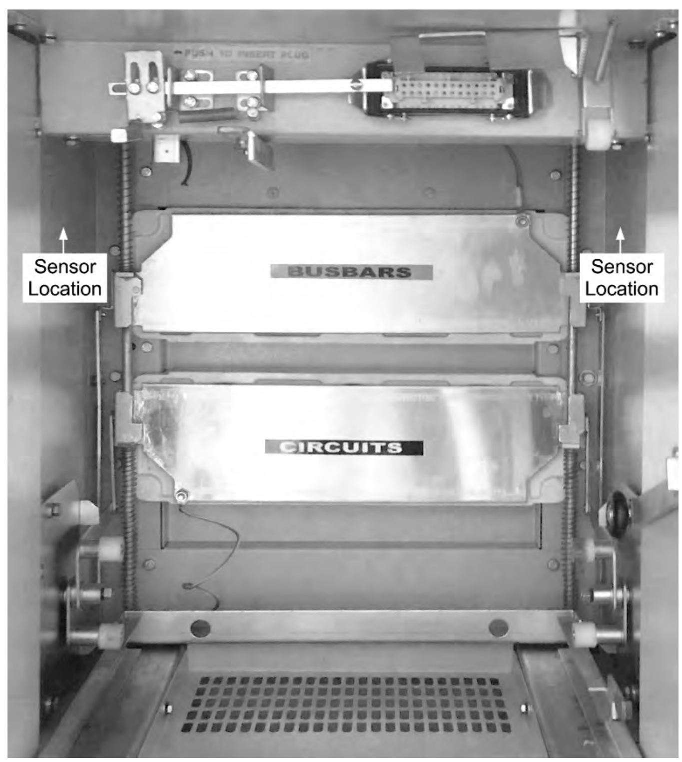

Fig. 11. Point Sensor Locations in Breaker Compartment of 11 kV Outgoing Switchgear Panel

Fig. 12 shows two point sensors installed in the cable compartment of an 11 kV switchgear panel.

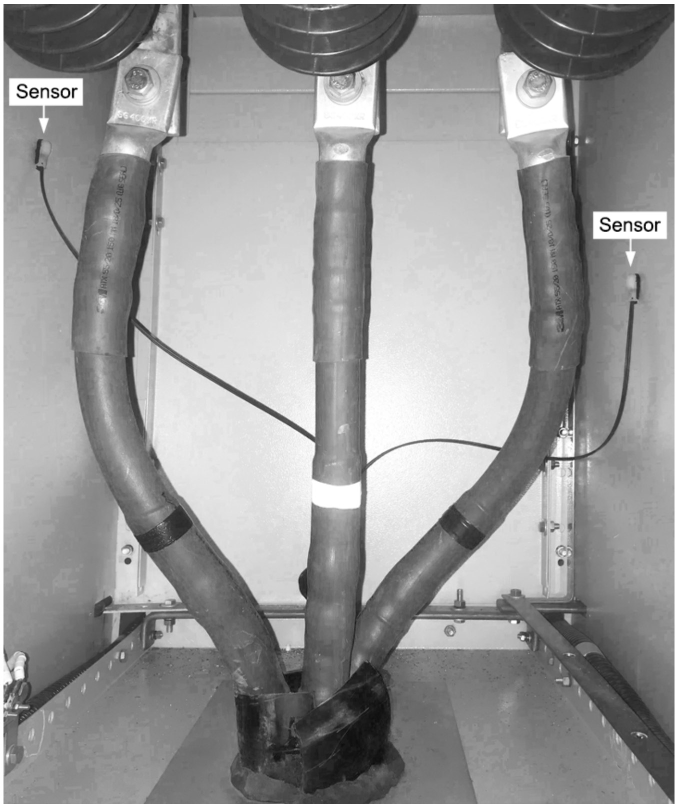

Fig. 12. Point Sensors Installed in Cable Compartment of 11 kV Outgoing Switchgear Panel

Bus compartment sensor installation is not pictured.

B. 415 V Switchboard Light Sensor Installation

In addition to the 11 kV outgoing feeders, there are four 415 V incoming feeders that emanate from four isolation transformers. (These are Transformers 1 through 4 shown in Fig. 8.) In each 415 V switchboard node, two point sensors and one bare-fiber sensor are installed for arc-flash detection. The two point sensors are placed on either side of the breaker chamber and the bare-fiber sensor is placed in busbar chamber to cover the entire busbar section.

A total of eight point sensors and four bare-fiber sensors are used in the four nodes of the 415 V switchboard. Fig. 13 shows the two point sensors in the breaker compartment of a 415 V switchboard node.

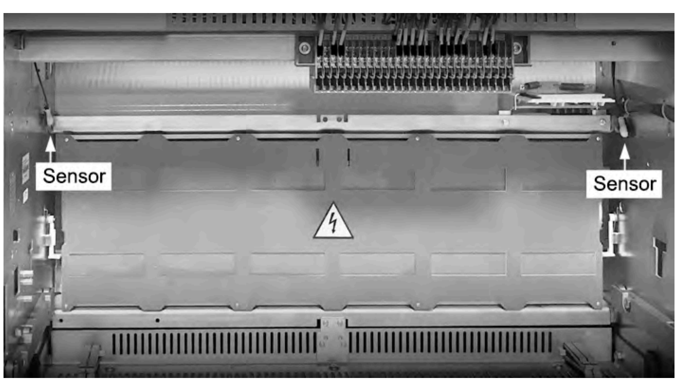

Fig. 13. Point Sensors in Breaker Compartment of 415 V Switchboard

Fig. 14 shows the bare-fiber sensor that is located around the perimeter of the busbar section of a 415 V switchboard node.

Fig. 14. Bare-Fiber Sensor Around Busbar Perimeter of 415 V Switchboard

VIII. Arc-Flash Detection System Settings and Testing for TPDDL Facility

Prior to testing, engineers checked the wiring diagram and routing of all light sensors in the system (point sensors and bare-fiber sensors).

The relays in the arc-flash detection system use high-speed overcurrent elements that are set at twice the expected maximum load current of the feeder. Each of the arc-flash detection sensors is also associated with a TOL element in the relay. The TOL element has two settings, which are used to define the type of the attached sensor and the TOL pickup value.

Table VI and Table VII show the relay settings associated with the high-speed overcurrent element and the light intensity monitored by the sensors. The threshold values for the light intensity settings are set by taking into account the ambient light intensity measured by the installed sensors and relay.

Table VI
Relay Settings for 11 kV Switchgear

Relay Setting	Threshold Value
Overcurrent	1.5 A secondary
Point Sensor 1 light intensity	3%
Point Sensor 2 light intensity	3%
Point Sensor 3 light intensity	3%
Point Sensor 4 light intensity	3%

TABLE VII
RELAY SETTINGS FOR 415 V SWITCHBOARD

Relay Setting	Threshold Value
Overcurrent	7 A secondary
Point Sensor 1 light intensity	3%
Point Sensor 2 light intensity	3%
Bare-Fiber Sensor 3 light intensity	1%

The detection system testing used a secondary injection kit as a current source and a camera flash as a light source (Fig. 15), with both applied simultaneously to simulate an arc-flash event.

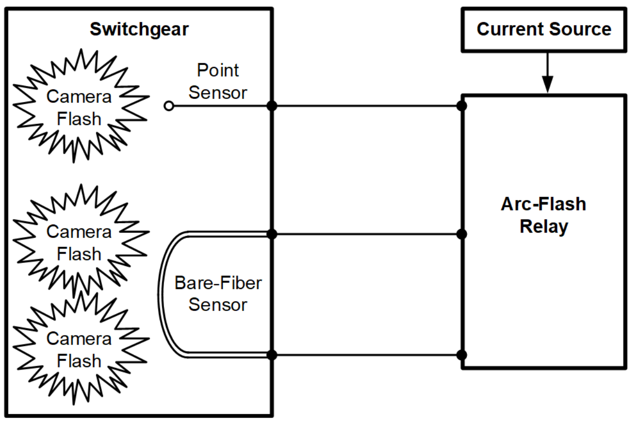

Fig. 15. Testing Configuration for Arc-Flash Detection System

IX. ARC-FLASH EVENT ANALYSIS

The arc-flash event occurred when Transformer 4 was energized from the 11 kV outgoing feeder. While testing the Node 4 battery charger, TPDDL engineers tried to charge the 415 V bus by closing the 415 V incomer breaker. During bus energization, arc-flash protection in the incomer relay operated.

On analysis of the event report captured by the relay, engineers found that the relay measured a fault current of about 39.44 kA in Phase A and 37.88 kA in Phase B during the arc-flash event. Fig. 16 shows the recorded magnitude of the peak current during the fault.

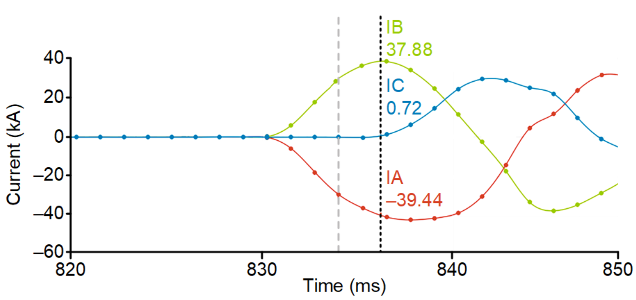

Fig. 16. Current Magnitude During Arc-Flash Event

Because the fault was in the vicinity of the two point sensors placed on the breaker chamber, these point sensors were able to sense 100 percent arc-flash light during the fault. Fig. 17 shows the light intensity reported by the nearby sensors.

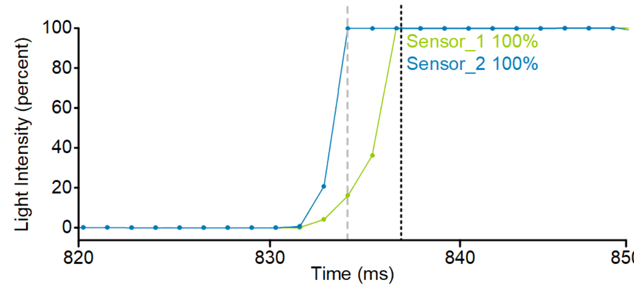

Fig. 17. Light Intensity During Arc-Flash Event

Further investigation was carried out at the 415 V Node 4 switchboard to identify the cause. Engineers found a stray bolt on the busbar led to the fault. The bolt may have been left on the busbar cover by workers during switchboard installation.

When the breaker closed during testing, the vibrations caused by the breaker made the loose bolt drop from the busbar insulation cover and contact the bare copper busbar at the outgoing breaker terminal L-joint, as shown in Fig. 18. This L-joint located at the back of the breaker connects the busbar section to the breaker. The bolt shorted Phase A and Phase B of the busbar. Fig. 19 and Fig. 20 are post-fault photographs of the bolt and the breaker output terminal.

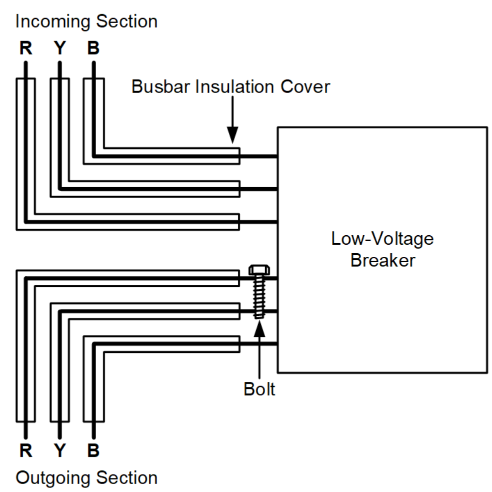

Fig. 18. Faulted Breaker Connection With Bolt on Busbar

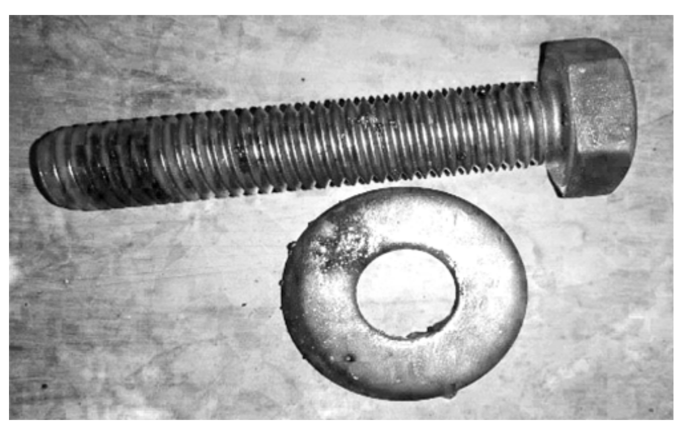

Fig. 19. Stray Bolt and Washer Found Near Fault Location

Fig. 20. Fault Location at Breaker Output Terminal

The high-intensity incident energy spread the arc, causing the phase-to-phase fault to develop into a three-phase fault. The arc, generated on the 415 V breaker output terminals, also impacted the 415 V input terminals, because the output and input terminals are not in separate compartments.

The 415 V incomer relay arc-flash protection operated in 3.76 ms, as shown in Fig. 21. The breaker took an additional 60 ms to open and clear the fault on the output terminal of the 415 V incomer feeder breaker.

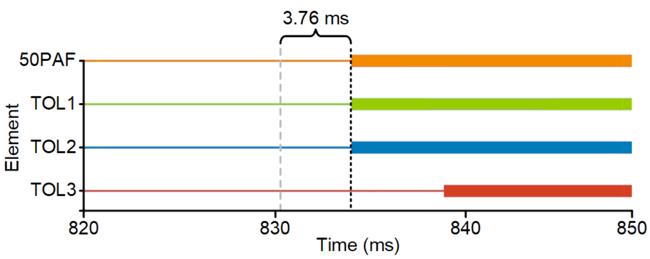

Fig. 21. Operating Time From Event Report

After the 415 V breaker opened, the peak fault current value decreased from 39.88 kA to 24 kA in the 415 V level and from 1.69 kA to 1.1 kA in the 11 kV level. However, the arcing current on the 415 V incomer breaker input terminal was interrupted by the relay at the 11 kV outgoing feeder. The 11 kV outgoing feeder operated on IDMT overcurrent to isolate the fault. The total fault-clearing time was 191.06 ms including the 11 kV breaker opening time, as shown in Fig. 22.

The 11 kV breaker was supposed to be tripped by the arc-flash protection from the 415 V switchgear, because a direct transfer trip protection scheme was implemented in the system design: a high-speed output contact from the 415 V incomer relay was configured to trip the 11 kV outgoing breaker.

However, the wiring connections associated with this inter-tripping scheme between the 415 V breaker and the 11 kV outgoing breaker had not yet been established during the testing of the system. This resulted in the 415V breaker input terminal fault to be fed from the upstream transformer. The subsequent relay on the 11 kV outgoing feeder tripped on IDMT overcurrent protection after 191.06 ms.

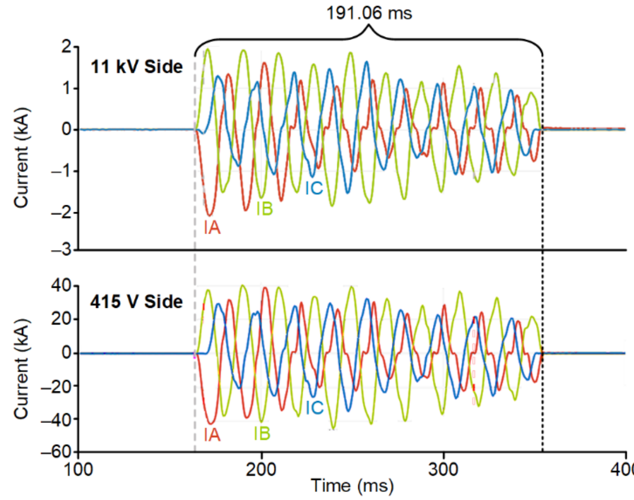

Fig. 22. Fault-Clearing Time From Event Report

The incident energy and the arc-flash boundary could have been reduced further if the inter-tripping wiring connections had been established prior to the fault. If the inter-tripping scheme had been active during the arc-flash event, it would have reduced the incident energy from 23.22 cal/cm^2 to 5.073 cal/cm^2 (a reduction percentage of 78.1 percent) and significantly reduced the arc-flash boundary from 4.57 m to 1.62 m. Therefore, based on this arc-flash event, the inter-tripping scheme is being implemented at the facility.

X. Conclusion

For the arc-flash event that occurred during the commissioning test at the TPDDL facility, the installed relays with arc-flash protection greatly reduced fault-clearing time for the fault on the 415 V switchboard. Because of the extremely fast operation, damage to the 415 V busbar was minimal. The incident energy of the fault could have been further mitigated by reducing the fault-clearing time using an inter-tripping scheme between the 11 kV and 415 V sections.

The arc-flash event at this facility illustrates the importance of implementing an arc-flash detection system along with an inter-tripping scheme in applications where breaker input and output terminals are in the same compartment with limited clearance space.

Arc-flash protection with high-speed overcurrent elements saved both equipment and human life during this event. The installation of an arc-flash detection system and an inter-tripping scheme makes the TPDDL energy storage facility a safer place to work for operation and maintenance personnel.

XI. References

[1] NFPA 70E, Standard for Electrical Safety in the Workplace, 2018.

[2] D. Johnson, "Arc Flash Statistics," Industrial Safety & Hygiene News Magazine, May 2013. Available: https://www.ishn.com/articles/96001-arc-flash-statistics.

[3] IEEE 1584, IEEE Guide for Performing Arc-Flash Hazard Calculations.

[4] M. Zeller and G. Scheer, "Add Trip Security to Arc-Flash Detection for Safety and Reliability," proceedings of the 35th Annual Western Protective Relay Conference, Spokane, WA, October 2008.

[5] J. Buff and K. Zimmerman, "Application of Existing Technologies to Reduce Arc-Flash Hazards," proceedings of the 33rd Annual Western Protective Relay Conference, Spokane, WA, October 2006.

[6] A. Guzmán, C. Labuschagne, and B Qin, "Reliable Busbar and Breaker Failure Protection with Advanced Zone Selection," proceedings of the 31st Annual Western Protective Relay Conference, Spokane, WA, October 2004.

[7] B. Hughes, V. Skendzic, D. Das, and J. Carver, "High-Current Qualification Testing of an Arc-Flash Detection System," proceedings of the 9th Annual Clemson University Power Systems Conference, Clemson, SC, March 2010.

XII. Biographies

Manibhushan Prasad received his bachelor of engineering degree in electrical engineering from the National Institute of Technology in 2004. He joined Tata Power Delhi Distribution Limited in 2004 as a graduate engineer trainee and is presently working as a group lead senior manager in the protection, testing and automation division, involved in the development, design, implementation, commissioning, and maintenance of numerous protection- and automation-based projects. Presently he handles protection and testing for about 30 substation projects (66 kV, 33 kV, and 11 kV).

Mohanraj Perumalsamy received his bachelor of engineering degree in electrical engineering from Anna University in 2012. He started his professional career with Voltech Engineers Private Limited as a protection engineer. He joined Schweitzer Engineering Laboratories, Inc. in 2016 as an application engineer I and is currently working as an application engineer II in India. He has been involved in substation and generator protection; application engineering; and testing and commissioning protection and control solutions.

Shripad Kapse received his bachelor of engineering degree in electrical engineering, with honors, from Visvesvaraya Technological University in 2011 and received his postgraduate diploma in transmission and distribution systems from the National Power System Institute in 2012. He started his professional career with Easun Reyrolle Limited as an application engineer. He joined Schweitzer Engineering Laboratories, Inc. in 2015 and is currently working as an application engineer in India. He has been involved in fast motor bus transfer solutions; disturbance recorders; application engineering; and testing and commissioning protection and control solutions.

Chethan Kumar Barikar received his bachelor of engineering degree in electrical and electronics engineering from Visvesvaraya Technological University in 2009. He joined Schweitzer Engineering Laboratories, Inc. (SEL) in 2010 as an associate protection engineer. He is presently working as a lead project engineer in SEL Engineering Services, Inc. and is involved in the development, design, implementation, and commissioning of numerous protection- and automation-based projects.

Deepak Srivastava received his bachelor of engineering degree in electrical engineering from Nagpur University in 2008. He worked as a protection engineer for Sterling and Wilson Limited and Easun Reyrolle Limited for six years. He joined Schweitzer Engineering Laboratories, Inc. (SEL) in 2017 as a protection engineer. He is presently working as a project engineer in SEL Engineering Services, Inc. and is involved in the tendering, design, implementation, and commissioning of numerous protection-based projects.

Ricardo Abboud received his B.S.E.E. degree in electrical engineering from Universidade Federal de Uberlândia, Brazil, in 1992. In 1993, he joined CPFL Energia as a protection engineer. In 2000, he joined Schweitzer Engineering Laboratories, Inc. (SEL) as a field application engineer in Brazil, assisting customers in substation protection and automation. In 2005, he became the field engineering manager, and in 2014, he became the engineering services manager. In 2016, he transferred to Pullman, Washington, and is currently an international technical manager. He is a certified instructor at SEL University, and has authored and coauthored several technical papers.

20190905 • TP6929-01